

HOW BLACK ARE BLACK HOLE CANDIDATES?

STANLEY L. ROBERTSON¹ AND DARRYL J. LEITER²

Draft version December 24, 2018

ABSTRACT

In previous work we found that many of the spectral properties of x-ray binaries, including both galactic black hole candidates (GBHC) and neutron stars, were consistent with the existence of intrinsically magnetized central objects. Here we review and extend the observational evidence for the existence of intrinsically magnetized GBHC and show that their existence is consistent with a new class of solutions of the Einstein field equations of General Relativity. These solutions are based on a strict adherence to the Principle of Equivalence, which prevents the time-like geodesics of physical matter from becoming null on trapped surfaces of infinite red shift. The new solutions emerge from the fact that the structure and radiation transfer properties of the energy-momentum tensor on the right hand side of the Einstein field equations must have a form that is consistent with this Principle of Equivalence requirement. In this context, we show that the Einstein field equations allow the existence of highly red shifted, magnetospheric, eternally collapsing objects (MECO) which do not have trapped surfaces which lead to event horizons. Since MECO lifetimes are many orders of magnitude greater than a Hubble time, they provide an elegant and unified framework for understanding the broad range of observations associated with GBHC and active galactic nuclei.

Subject headings: Accretion, Black Holes, Active Galaxies, Stars: neutron, Stars: novae, X-rays: stars

1. INTRODUCTION

In previous work (Robertson & Leiter 2002) we presented evidence for the existence of intrinsic magnetic moments in galactic black hole candidates (GBHC). We proposed that this observational result was consistent with the idea that the fundamental structure of General Relativity allows the existence of eternally collapsing objects (ECO) without event horizons (Mitra, 2000, 2002). Since the energy-momentum tensor of the right hand side of the Einstein field equations serves as both a source of curvature and a generator of equations of motion of matter, any constraints on the latter will impact the former. In this regard, the Principle of Equivalence (POE) requirement that the time-like geodesics of matter cannot become null is a constraint that must be encompassed by elements included in the energy-momentum tensor. In Section 2 we show that strict adherence to the POE implies that the Einstein field equations possess physical solutions consistent with the existence of highly red shifted, magnetospheric eternally collapsing objects (MECO) in which trapped surfaces of infinite redshift leading to event horizons cannot form. Unlike the cold, catalyzed matter of neutron stars, with only limited masses that can be supported by degeneracy pressure, MECO are hot and radiatively supported while slowly collapsing. Since the MECO solutions have observable lifetimes which are many orders of magnitude greater than a Hubble time, their existence as the central compact component of active galactic nuclei (AGN) is compatible with the broad range of observations associated with GBHC and AGN.

This work is intended as a first introduction to MECO phenomena. We hope to make the existence of MECO plausible and show that they fit very comfortably within

the complex phenomenology of compact astrophysical objects, while necessarily leaving many important and difficult issues for later work. In Sections 3 and 4, we first consider some general properties of quiescent and active MECO. In Section 5 we examine the compatibility of MECO models of GBHC and AGN with a variety of astrophysical observations. We find that compatibility with observations requires that the MECO rates of rotation be relatively slow. We find that generally diamagnetic accreting plasma interacting with the magnetic field of a MECO via an accretion disk provides an elegant and unified framework for understanding compact x-ray sources. In particular, the MECO model accounts for the high state ‘ultrasoft’ radiation (White & Marshall 1984), the high state power law emissions, the spectral state switch, including the radio-loud and radio quiet states, low state jets and equatorial outflows, and the quiescent luminosities of GBHC.

There is a plethora of piece meal black hole models of these various phenomena. For example, comptonizing coronae near event horizons, bulk flow comptonization, accretion disk coronae, and magnetic flares on accretion disks have all been invoked to explain the hard spectral tail of black hole GBHC. Radiatively inefficient advective flows at high accretion rates have been proposed to explain their quiescent power-law emissions while overlooking the obvious fact that such flows do not occur for neutron star binaries. Since there is no unified black hole model, while the MECO model provides a comprehensive and unified approach, the replacement of black holes by MECO represents a paradigm shift in the astrophysics of compact objects. To believe in the existence of trapped surfaces and event horizons is to believe that nature has provided a way to accelerate particles with non-zero rest mass to

¹Dept. of Physics, Southwestern Oklahoma State University, Weatherford, OK 73096

²FSTC, Charlottesville, VA 22901

exactly the speed of light. The POE implies that this is impossible and the issue can be settled by observations of magnetospheric phenomena. MECO have magnetic moments, black holes do not.

2. PRINCIPLE OF EQUIVALENCE AND MECO

In General Relativity the Principle of Equivalence (POE) requires that Special Relativity must hold locally for all freely falling time-like observers. This ‘medium-strong’ form (Wheeler & Ciufolini 1995) of the principle can be expressed as a tensor relationship, which means that in a general curved spacetime, physical matter must follow time-like world lines such that the associated invariant line interval obeys

$$ds^2 = g_{ij}dx^i dx^j = c^2 d\tau^2 = \frac{c^2 dt^2}{(1+z)^2} > 0 \quad (1)$$

where $(1+z)$ is the red shift given by

$$(1+z) = \frac{dt}{d\tau} \quad (2)$$

The POE requires that the proper time $d\tau$ along time-like world lines of physical matter must exist and world lines of massive particles must always remain time-like, which implies that

$$1/(1+z) > 0 \quad (3)$$

on all time-like world lines over all regions of spacetime. Therefore the matter equations of motion determined by the Bianchi Identity $T^{\mu\nu};\nu = 0$, where $T^{\mu\nu}$ is the energy-momentum tensor, must always describe time-like motion. This acts as a constraint on the radiation transport described by the energy momentum tensor on the right hand side of the Einstein equation $G^{\mu\nu} = 8\pi T^{\mu\nu}/c^4$.

It is clear that a strict application of the POE to the solutions of the Einstein field equations in General Relativity, implies that trapped surfaces leading to event horizons cannot be physically realized through the time-like collapse of radiating physical matter. If an event horizon were to form during collapse, this would require the time-like world line of the collapsing matter to become null in violation of the POE. On the other hand, there is an enormous volume of literature concerning black holes that is built entirely on the assumption that trapped surfaces exist. In previous work we have presented observational evidence against this assumption. Here we provide a specific MECO model of compact objects that is in accord with this POE requirement.

Although the existence of objects compact enough to qualify as black hole candidates is beyond question, no compelling evidence for the existence of event horizons has been found. In fact, It has recently been argued (Abramowicz, Kluzniak & Lasota 2002), that proof is fundamentally impossible, precisely because highly red shifted, compact objects cannot be excluded. The reverse is not true, however, for it may be possible to prove that these compact objects possess intrinsic magnetic moments.

Let us now consider the time-like collapse of a compact, radiating plasma of mass M_s , surrounded by a physical surface, R_s in contact with the plasma. Then generalizing from earlier work, (Hernandez & Misner 1966; Lindquist, Schwartz & Misner 1965; Lindquist 1966, Misner 1965) the

co-moving metric associated with this situation will have the general form:

$$ds^2 = A^2 c^2 dt^2 + 2Dc dt dR - B^2 dR^2 - R^2(t_r)(d\theta^2 + \sin^2\theta d\phi^2) \quad (4)$$

where $t_r = t - r/c$ is the retarded time.

Substitution of the metric into the Einstein equation $G^{\mu\nu} = 8\pi T^{\mu\nu}/c^4$, with an energy momentum tensor $T^{\mu\nu}$ whose form describes the radiating plasma collapse leads to a set of equations from which, with appropriately chosen boundary conditions, the functions $A(r,t_r)$, $B(r,t_r)$, and $D(r,t_r)$ can be determined. However, independently of the detailed form of the $T^{\mu\nu}$, the first integral of the mixed time-time component of the Einstein equation gives the proper time of the collapsing surface synchronized along world lines of the collapsing plasma on the surface, R_s as

$$d\tau_s = dt_r/(1+z_s) = dt_r(\Gamma_s + U_s/c) > 0 \quad (5)$$

where z_s is the red shift of the radiating collapsing surface, $t_r = t - R_s/c$ and

$$\Gamma_s = (1 - \frac{R_{schw}}{R_s} + (\frac{U_s}{c})^2)^{1/2}. \quad (6)$$

Here $U_s = (\frac{dR}{dt})_s < 0$ is the proper time rate of change of the radius associated with the invariant circumference of the collapsing surface, R_s and $R_{schw} = 2GM_s/c^2$, where $M_s(r,t)$ is the total mass contained within the surface as defined by the general formula:

$$M_s(R_s, t) = \int (T_0^0 \Gamma dV)_s. \quad (7)$$

Here $\Gamma_s = (\frac{dR}{dt})_s$ and dV is the proper volume element, $dV = 4\pi R^2 dl$. Here dl is the proper length inside and on the surface $R = R_s$ and is given by $dl = BdR$.

Since M_s is being radiated away by photon emission then the luminosity at infinity is given by

$$L_\infty = -c^2 \frac{dM_s}{dt_r} = -c^2 \frac{dM_s}{d\tau} (1+z_s) \quad (8)$$

and the proper time rate of change of the Schwarzschild radius with the mass M_s inside is

$$U_{schw} = (\frac{dR_{schw}}{d\tau})_s = \frac{2G}{c^2} \frac{dM_s}{d\tau_s} < 0 \quad (9)$$

Now since the POE requires that the collapse of the radiating physical surface must always be time-like, it follows that the element of proper time synchronized along the radial world line of a fluid element on the boundary of the collapsing fluid must always obey $d\tau_s > 0$. Hence this requires that (see Appendix A)

$$d\tau_s = dt_r((1 - \frac{R_{schw}}{R_s} + (\frac{U_s}{c})^2)^{1/2} + \frac{U_s}{c}) = \frac{dt_r}{1+z_s} > 0, \quad (10)$$

Hence from Equation (10) we see that for $U_s < 0$, the POE requires that the ‘no trapped surface condition’, $R_{schw}/R_s < 1$ must hold.

For a collapsing plasma emitting particles at the local Eddington limit, L_{edd} , the local radial collapse velocity of

the surface, U_s essentially vanishes. Under these conditions the POE requirement $R_s > R_{schw}$ for the collapse process, when differentiated with respect to proper time, implies that $0 = -U_s < -U_{schw}$ is dynamically satisfied by the equations of motion of the matter. It follows that the POE requires that the physical dynamics associated with the general relativistic radiation transfer process must prevent the collapsing surface from passing through the Schwarzschild radius. In Appendix A we show in detail that when the Eddington limit is established at red shift $(1+z) = (1+z_{edd})$, the POE applied to the Einstein Equation implies that the time-like collapsing radiating surface of the MECO lies outside of the Schwarzschild radius of the collapsing object and remains that way for the duration of the Eddington limited collapse process. In Appendix B we show that if $(L(escape)_{edd})_s$ is the luminosity generated within which escapes from the collapsing surface, then the red shift at which an Eddington balance will be achieved is given by

$$1 + z_{Edd} = \frac{\kappa(L(escape)_{edd})_s}{4\pi GM_s c}. \quad (11)$$

Here G is the Newtonian gravitational force constant and κ the plasma opacity. Then in terms of the quantity $U_{schw} = \frac{dR_{schw}}{d\tau}$, this implies that

$$\frac{U_{schw}}{c} = \frac{-2G(L(escape)_{edd})_s}{c^5(1+z_{edd})} < \frac{U_s}{c} \quad (12)$$

consistent with the POE requirement that $R_{schw} < R_s$ must be maintained by the physical forces which act during the collapse process.

If one naively attributes the Eddington limit luminosity to purely thermal processes, one quickly finds that the required MECO surface temperatures would be so high that photon energies would be well above the pair production threshold and extensive electron-positron pair production would occur due to photon-photon collisions. Thus the MECO surface region must be dominated by a pair plasma, and at a temperature not greatly different from the $6 \times 10^9 K$ threshold for photon-photon collisions to produce pairs (Pelletier & Marcowith 1998). In addition, a substantial magnetic field is necessary in order to confine the pair plasma. For a source of radius R and radiating luminosity L , a balance of radiative and magnetic stresses would require a magnetic field strength of $B > \sqrt{4L/\pi R^2 c} \sim 10^8$ gauss for a $10 M_\odot$ Eddington limit GBHC. For an Eddington limit L increasing as $1+z$, as implied by equation 11, the surface magnetic field would need to be larger by the factor of $\sqrt{1+z}$. For the large red shifts contemplated in this work, it will be necessary to consider very large surface magnetic fields. Pelletier & Marcowith (1998) have shown that the energy of magnetic perturbations in pair plasmas can be preferentially transferred to radiation, rather than causing particle acceleration for equipartition magnetic fields. The radiative power of an equipartition pair plasma is proportional to

B^4 because the pair density is proportional to B^2 , in addition to a synchrotron energy production proportional to B^2 . Because of this extremely efficient photon production mechanism, the radiation temperature is buffered. When particle kinetic pressure is in equipartition with magnetic pressure, the field also exceeds that required to confine the plasma, thus stability is maintained.

In an extremely compact object, the particle kinetic pressure might be as high as $\rho c^2/3$. If we take $\rho = M/(4\pi R^3/3)$, $R \approx 2GM/c^2$ and equate the magnetic and particle kinetic pressures, we obtain $B_{equip} = c^4/(4MG^{3/2}) = 6 \times 10^{18}/m$ gauss, where $m = M/M_\odot$ is the mass in solar mass units. Thus the dynamic condition required for an Eddington limited stationary equilibrium to initially occur at red shift $(1+z_{edd})$ during the MECO plasma collapse process is that the MECO must contain an equipartition magnetic field with energy density $B^2/8\pi$ that is comparable to the particle kinetic pressure. Then the existence and stability of the $U_s = 0$, Eddington limited MECO regime is guaranteed because the intrinsic, equipartition magnetic field is the primary source of luminosity. Since this luminosity is not confined to the core of the MECO it will not be trapped, as occurs with neutrinos, however, the radiation should be thermalized by the optically thick environment from which it escapes. Finally, we note that although there have been many numerical computations that apparently show the formation of trapped surfaces, to our knowledge none have had sufficient numerical resolution to examine this extreme red shift regime nor have they considered the emergent properties of equipartition magnetic fields and pair plasmas at high red shift. As we shall see, an electron-positron pair atmosphere of a MECO is an extremely significant structure that conveys radiation from the MECO surface to a zone with a much lower red shift and larger escape cone from which it escapes. In order to capture it within a numerical grid, a grid point spacing of at least $10^{-8} R_g$ would be needed, where $R_g = GM/c^2$ is the gravitational radius.

The strength of the intrinsically generated magnetic fields B_{env} observed in the distant environment around the MECO are reduced by a factor of $(1+z_{edd})$ from their values near R_s . The fields needed to produce jets in AGN are observed to be of the order $10^3 - 10^4$ gauss as judged from a distance. On the other hand, a distantly observed equipartition field would be $\sim 6 \times 10^{18}/(m(1+z_{edd}))$ gauss. This suggests that for an $m \sim 10^8$ AGN, the combined effect of mass scaling and red shift would need to reduce the surface field from 6×10^{18} gauss to 10^{3-4} gauss. This would require the MECO to have a red shift of $z \sim 10^7 - 10^8$. In previous work, (Robertson & Leiter 2002) we have found typical magnetic fields of a few times 10^{10} gauss for GBHC. These would require similar values of $z_{edd} \sim 10^8$, as well as $m \sim 10$. Therefore for both GBHC and AGN we find that

$$1 + z_{edd} = \frac{B_{equip}}{B_{env}} \sim 10^8. \quad (13)$$

3

The quiescent luminosity of a MECO originates deep

³An additional point of support for very large values of z concerns neutrino transport in stellar core collapse. If a diffusion limited neutrino luminosity of $\sim 10^{52}$ erg/s (Shapiro & Teukolsky 1983) were capable of briefly arresting the collapse, then the subsequent reduction of neutrino luminosity as neutrino emissions are depleted in the core would lead to a rapid adiabatic collapse until photon emissions reach an Eddington limit. At this point the photon luminosity would need to support a smaller and much more tightly gravitationally bound mass. An order of magnitude calculation of binding energy ($\sim Mc^2 \ln(1+z)$) indicates that when stable, an $m = 10$ MECO should be approximately 17 times

within its photon sphere. When distantly observed it is diminished by both gravitational red shift and a narrow exit cone. The gravitational red shift reduces the surface luminosity by $1/(1+z)^2$ while the exit cone further reduces the luminosity by the factor $27(1+z)^2 u^2 \sim 27(1+z)^2/4$ for large z . (See Appendix C). Here we have used

$$u = \frac{GM_s}{rc^2} = \frac{R_g}{r} = \frac{1}{2} \left(1 - \frac{1}{(1+z)^2}\right) \quad (14)$$

where r and z refer to the location from which photons escape. The net outflow fraction of the luminosity provides the support for the collapsing matter. The photons actually escape from the photosphere of a pair atmosphere.

3. THE QUIESCENT MECO

The fraction of luminosity from the MECO surface that escapes to infinity in Eddington balance is (Appendix B):

$$(L_{edd})_s = \frac{4\pi GM_s c(1+z)}{\kappa} = 1.27 \times 10^{38} m(1+z_s) \quad \text{erg/s} \quad (15)$$

In the last expression we have used $\kappa = 0.4 \text{ cm}^2/\text{g}$. The distantly observed luminosity is:

$$L_\infty = \frac{(L_{edd})_s}{(1+z_s)^2} = \frac{4\pi GM_s c}{\kappa(1+z_s)} \quad (16)$$

When radiation reaches the photosphere, where the temperature is T_p , the fraction that escapes is:

$$L_\infty = \frac{4\pi R_g^2 \sigma T_p^4}{u_p^2} \frac{27u_p^2}{(1+z_p)^4} = 1.56 \times 10^7 m^2 T_p^4 \frac{27}{(1+z_p)^4} \quad \text{erg/s} \quad (17)$$

where $\sigma = 5.67 \times 10^{-5} \text{ erg/s/cm}^2$ and subscript p refers to conditions at the photosphere. Equations 16 and 17 yield:

$$T_\infty = T_p/(1+z) = \frac{2.3 \times 10^7}{(m(1+z_s))^{1/4}} \quad \text{K}. \quad (18)$$

To examine typical cases, a $10M_\odot$, $m = 10$ GBHC modeled in terms of a MECO with $z \sim 10^8$ would have $T_\infty = 1.3 \times 10^5 \text{ K} = 0.01 \text{ keV}$, a luminosity of $L_\infty = 1.3 \times 10^{31} \text{ erg/s}$, and a spectral peak at 220 \AA , in the photoelectrically absorbed deep UV. For an $m=10^7$ AGN, $T_\infty = 4160 \text{ K}$, $L_\infty = 1.3 \times 10^{37} \text{ erg/s}$ and a spectral peak in the near infrared at 7000 \AA . Considering these emission rates as indicators of the rate that high red shift MECO would lose mass, their apparent radiative lifetimes would be millions of Hubble times. (See Appendix A & B for exact lifetime results). Hence passive MECO without active accretion disks, although not black holes, have lifetimes much greater than a Hubble time and emit highly red shifted quiescent thermal spectra that would be quite difficult to observe. There are additional power law components of similar magnitude that originate as magnetic dipole spin-down radiation (see below).

less massive than at the point of loss of neutrino support. (This has obvious, important consequences for hypernova models of gamma ray bursters.) A new photon Eddington balance would thus require an escaping luminosity reduced by a factor of 17 and also reduced by the ratio (σ_T/σ_ν) , where $\sigma_T = 6.6 \times 10^{-25} \text{ cm}^2$ is the Thompson cross section and $\sigma_\nu = 4.4 \times 10^{-45} \text{ cm}^2$ is the neutrino scattering cross-section. (This would be the opacity ratio as long as particles of the same mass are being supported by both photons and neutrinos.) Thus $L_\infty \sim 8 \times 10^{32} \text{ erg/s}$ would be required. For a $7 M_\odot$ GBHC, this would require $1+z \sim 10^9$. It is of some interest that neutrinos with non-zero rest mass would be trapped inside the photon sphere anyway.

⁴We consider the pair atmosphere to exist external to the Meco. In exterior Schwarzschild geometry, the hydrostatic balance equation within the MECO atmosphere is $\frac{\partial p}{\partial r} = -\frac{\partial \ln(g_{00})}{2\partial r}(p + \rho c^2)$, where $g_{00} = (1 - 2u)$ and $\rho c^2 \ll p$. This integrates to $p/(1+z) = \text{constant}$.

Escaping radiation passes through a pair plasma atmosphere that can be shown, *ex post facto* (See Appendix F), to be radiation dominated throughout. Under these circumstances, the radiation pressure within the equilibrium atmosphere obeys $P_{rad}/(1+z) = \text{constant}$.⁴ Thus the relation between surface and photosphere temperatures is $T_s^4/(1+z_s) = T_p^4/(1+z_p)$. At the MECO surface, we expect a pair plasma temperature of $T_s \approx m_e c^2/k \sim 6 \times 10^9 \text{ K}$ because an equipartition magnetic field effectively acts as a thermostat which buffers the temperature of the optically thick synchrotron radiation escaping from the MECO surface (Pelletier & Marcowith 1998). But since $T_\infty = T_p/(1+z_p)$, we have that

$$T_p = T_s \left(\frac{T_s}{T_\infty(1+z_s)}\right)^{1/3} = \frac{1.76 \times 10^9}{(m(1+z_s))^{1/12}} \quad \text{K} \quad (19)$$

For $1+z_s = 10^8$ and $m = 10$ GBHC, this yields a photosphere temperature of $3.1 \times 10^8 \text{ K}$, from which $(1+z_p) = 2400$. An AGN with $m = 10^7$ would have a somewhat cooler photosphere at $T_p = 9.9 \times 10^7 \text{ K}$, but with a red shift of 24000. If surface temperature for an AGN MECO were somewhat lower than $6 \times 10^9 \text{ K}$, the pair mass density could be below the mean density of matter in the AGN. Thus it becomes plausible to consider that AGN might be predominately pair plasma with relatively small baryonic content.

4. AN ACTIVELY ACCRETING MECO

From the viewpoint of a distant observer, accretion would deliver mass-energy to the MECO, which would then radiate most of it away. The contribution from the central MECO alone would be

$$L_\infty = \frac{4\pi GM_s c}{\kappa(1+z_s)} + \frac{\dot{m}_\infty c^2}{1+z_s} (e(1+z_s) - 1) = 4\pi R_g^2 \sigma T_p^4 \frac{27}{(1+z_p)^4} \quad (20)$$

where $e = E/mc^2 = 0.943$ is the specific energy per particle available after accretion disk flow to the marginally stable orbit radius, r_{ms} . Assuming that \dot{m}_∞ is some fraction, f , of the Newtonian Eddington limit rate, $4\pi GM_s c/\kappa$, then

$$1.27 \times 10^{38} \frac{m\eta}{1+z_s} = (27)(1.56 \times 10^7) m^2 \left(\frac{T_p}{1+z_p}\right)^4 \quad (21)$$

where $\eta = 1 + f((1+z_s)e - 1)$ includes both quiescent and accretion contributions to the luminosity. Due to the extremely strong dependence on temperature of the density of pairs, (see Appendix F) it is unlikely that the temperature of the photosphere will be greatly different from the $3.1 \times 10^8 \text{ K}$ found previously for a typical GBHC. Assuming this to be the case, along with $z = 10^8$, $m = 10$, and $f = 1$, we find $T_\infty = T_p/(1+z_p) = 1.3 \times 10^7 \text{ K}$ and

$(1+z) = 24$, which indicates considerable photospheric expansion. The MECO luminosity would be approximately $L_\infty = 1.2 \times 10^{39}$ erg/s. For comparison, the accretion disk outside r_{ms} (efficiency = 0.057) would produce only 6.8×10^{37} erg/s. Thus the high accretion state luminosity of a GBHC would originate primarily from the central MECO. A substantial fraction of the softer thermal luminosity would be Compton scattered to higher energy in the plunging flow inside r_{ms} . The thermal component would be ‘ultrasoft’ with a temperature of only 1.3×10^7 K. Even if a disk flow could be maintained all the way to the MECO surface, where a hot equatorial band might result, the escaping radiation would be spread over the larger area of the photosphere due to photons origins deep inside the photon orbit.

For radiation passing through the photosphere most photons would depart with some azimuthal momentum on spiral trajectories that would eventually take them across and through the accretion disk. Thus a very large fraction of the soft photons would be subject to bulk Comptonization in the inflow from the accretion disk. This contrasts sharply with the situation for neutron stars where few photons from the surface cross the disk. This could account for the fact that hard x-ray spectral tails are comparatively much stronger for high state GBHC. Our preliminary calculations for photon trajectories randomly directed upon leaving the photon sphere indicate that this process would produce a power law component with photon index greater than 2. These are difficult and important calculations for which the effects of multiple scattering are crucial. But they are beyond the scope of this paper, which is intended as a first description of the general MECO model.

5. DISCUSSION

Since the MECO model provides a framework for understanding most of the known spectral and timing features of compact x-ray sources, it is useful to recapitulate important features. The progression of configurations of accretion disk, magnetic field and boundary layer is shown in Figure 1. We begin with quiescence.

Quiescent luminosities that are generally 10 - 100 X lower for GBHC than for neutron stars (NS) have been claimed as evidence for the existence of event horizons. (Narayan et al. 1997, Garcia et al. 2002). In our MECO model, the quiescent emissions are magnetic dipole emissions that are characteristic of the magnetic moment and rate of spin of the central object. The lower quiescent luminosities of the GBHC are explained by their lower spin rates and (perhaps unobservably) low rates of quiescent emission from the central MECO.

In previous work (Robertson & Leiter 2002) we found that magnetic moments and spin rates could be determined from luminosities at the end points of a spectral hardening transition. This spectral state switch for NS in low mass x-ray binaries (LMXB) is due to a magnetic propeller effect (Ilarianov & Sunyaev 1975, Stella, White & Rosner 1986, Cui 1997, Zhang, Yu & Zhang 1997, Campana et al. 1998). The magnetic moments and spins were used to calculate the soft x-ray luminosity expected from low state spin-down. The results are recapitulated and extended in Table 1. The equations and methods of calculation are repeated, with minor corrections, in Appendix D. Calculated values of quiescent luminosity in Table 1 have

been corrected using a more recent correlation of spin-down energy loss rate and soft x-ray luminosity (Possenti et al. 2002), but results are otherwise unchanged from the previous work except for new additions. It is a very powerful confirmation of the propeller mechanism that spins are in good agreement with burst oscillation frequencies (Strohmayr 2000), magnetic moments are of similar magnitude to those determined from the spin-down of millisecond pulsars and the calculated quiescent luminosities are accurate.

Even though the quiescent surface luminosity of the MECO is very low, surface and the magnetospheric spin-down luminosities are capable of ablating the material in a quiescent accretion disk. For a GBHC, radiation at $\sim 10^{31}$ erg/s should raise the temperature of the optically thick inner disk above the ~ 5000 K instability temperature for hydrogen out to a distance of $r \sim 10^{10}$ cm. Therefore we expect the quiescent inner disk to be essentially empty with a large inner radius. The rate of mass flow ablated at the inner disk radius would only need to be $\sim 10^{13}$ g/s to produce the quiescent optical emission observed for GBHC and NS. The ablated material could escape if it reached the magnetic propeller region, which is confined to the light cylinder at a much smaller radius than that of the inner disk. This makes the MECO model compatible with the disk instability model of x-ray nova outbursts, which begin as ‘outside-in’ events in which substantial outer mass reservoirs have been observed to fill an accretion disk on the viscous timescale of a radially subsonic flow (Orosz et al. 1997).

In outburst, the disk flow first engages the magnetic field of the rotating central object near the light cylinder radius, $r_{lc} = c/2\pi\nu_s$. A boundary layer forms in the disk where matter of the inner radius is, at least temporarily, brought into co-rotation with the magnetosphere and loaded onto its field lines. Behind the disk boundary layer, the flow remains Keplerian and largely shielded by induced surface currents from the MECO magnetic field. As the inflow proceeds, the magnetosphere rejects it via the ‘propeller effect’ until the inner disk can push inside the co-rotation radius, r_c . From r_{lc} to r_c , the system is in the Low/Hard spectral state. Inside r_c , the propeller regime ends and matter of sufficient pressure can make its way inward. From quiescence to the light cylinder, the x-ray luminosity changes by a factor of only a few as the disk generates a soft thermal spectral component (which may be mistaken for surface radiation for NS.) From r_{lc} to r_c , the x-ray luminosity may increase by a factor of $\sim 10^3 - 10^6$. With inner disk inside r_c , the outflow and/or jets subside, the system becomes radio quiet, the photon index increases, and a soft thermal excess appears, both of which contribute to a softer spectrum, (e.g., see Fig. 3.3 of Tanaka & Lewin, p. 140), which may be even be described as ‘ultrasoft’ (White & Marshall 1984); particularly when the luminosity finally begins to decline.

Plasma flowing outward in the low state may depart in a jet, or as an outflow back over the disk as plasma is accelerated on outwardly curved magnetic field lines. Radio images of both flows have been seen (Paragi et al. 2002). Equatorial outflows could contribute to the low state hard spectrum by bulk Comptonization of soft photons in the outflow. This would accentuate the hardness by the depletion of the soft photons that would otherwise be observed

to arise from the disk. Such an outflow would be compatible with partial covering models for dipping sources, in which the hard spectral region seems to be extended and of small extent perpendicular to the disk (Church 2001, Church & Balucinska-Church 2001). Alternatively, an accretion disk corona might be a major contributor to the hard spectrum. For jet emissions, recent work (Corbel & Fender 2002) has shown that it may be possible to explain much of the broadband emissions from near infrared through soft x-rays as the power-law synchrotron emissions of compact jets, which have been directly imaged for some GBHC. Jets would be compatible with ‘lamp post’ reverberation models of AGN. It is noteworthy that strong ($> 10^8$) gauss magnetic fields have been found to be necessary at the base of the jets of GRS 1915+105 (Gliozzi, Bodo & Ghisellini 1999, Vadawale, Rao & Chakrabarti 2001). A recent study of optical polarization of Cygnus X-1 in its low state (Gnedin, Silantev & Titarchuk 2002) has found a magnetic field of $\sim 10^7$ gauss at the location of the optical emission. These fields at distances approximately equal to the co-rotation radius imply magnetic moments for both GRS 1915+105 and Cygnus X-1 that are in good agreement with those of Table 1. Either jet or equatorial outflows would appear to be manifestations of the interaction of the magnetic field of the central object and the accretion disk.

The Intermediate/Very High State occurs as the inner disk region moves inside r_c . This passage is often accompanied by substantial mass ejection in jets. It is followed by the Soft/High state in which accreting matter can flow to the central object. For matter sufficiently inside r_c , the propeller mechanism is incapable of stopping the flow, however, a boundary layer may form at the inner disk radius in this case. The need for a boundary layer for GBHC can be seen by comparing the magnetic pressure at the magnetosphere with the impact pressure of a trailing, subsonic disk. For example, for an average GBHC magnetic moment of $\sim 4 \times 10^{29}$ gauss cm³ from Table 1, the magnetic pressure at a r_{ms} radius of 6.3×10^6 cm for a $7 M_\odot$ GBHC would be $B^2/8\pi \sim 10^{17}$ erg/cm³. At a mass flow rate of $\dot{m} = 10^{18}$ g/s, which would be near Eddington limit conditions for a $7 M_\odot$ MECO, the inner disk temperature would be $T \sim 1.5 \times 10^7$ K. The disk scale height would be given by $H \sim rv_s/v_K \sim 0.0036r$, where $v_s \sim 4.5 \times 10^7$ cm/s and $v_K \sim 1.2 \times 10^{10}$ cm/s are acoustic and Keplerian speeds, respectively. The impact pressure would be $\dot{m}v_r/4\pi rH \sim 5.6 \times 10^5 v_r$ erg/cm³. It would require v_r in excess of the speed of light to let the impact pressure match the magnetic pressure. But since the magnetic field doesn’t move fast enough to eject the disk material inside r_c , matter piles up as essentially dead weight against the magnetopause and pushes it in. The radial extent of such a layer would only need to be $\sim kT/m_p g \sim 50$ cm, where m_p is the proton mass and g , the radial gravitational free fall acceleration, but it is likely distributed over a larger transition zone from co-rotation with the magnetosphere to Keplerian flow. The gas pressure in the inner part of the transition zone necessarily matches the magnetic pressure. We observe that if this be the case, radiation pressure in the disk, at $T = 1.5 \times 10^7$ K, is nearly three orders of magnitude below the gas pressure. Therefore a gas pressure dominated, thin, Keplerian disk with subsonic radial speed should continue all the way to

r_{ms} for a MECO. Similar conditions occur with disk radius inside r_c even for weakly magnetic NS. The nature of mass accumulations in the inner disk transition region and the way that they can enter the magnetosphere have been the subject of many studies, (e.g., Spruit & Taam 1990).

In the case of NS, sufficiently high mass accretion rates can push the magnetopause into the star surface. At this point the hard apex of the right side of the horizontal branch of the ‘Z’ track in the hardness/luminosity diagram is reached. It has recently been shown (Muno et al. 2002) that the distinction between ‘atoll’ and ‘Z’ sources is merely that this point is reached near the Eddington limit for ‘Zs’ and at perhaps $\sim 10 - 20\%$ of this luminosity (Barrett & Olive 2002) for the less strongly magnetized ‘atolls’. Atolls rarely reach such luminosities. For MECO based GBHC, one would expect a relatively constant ratio of hard and soft x-ray ‘colors’ (e.g. van der Klis, et al.) after the inner disk crosses r_c and the flow reaches the photon orbit.

For the more massive GBHC and AGN, the disk, when inside r_c , is not masked by outflow and the disk itself shows a soft thermal spectral component. However, as we have shown in Section 4, significantly brighter radiation of similar temperature arises from matter plunging inside r_{ms} and reaching the MECO.

An observer at coordinate, r , inside r_{ms} , would find the radial infall speed to be $v_r = \frac{\sqrt{2}}{4}c(6u - 1)^{3/2}$, where $u = GM/rc^2 = R_g/r$ (see Appendix C) and the Lorentz factor for a particle spiraling in from $6R_g$ would be $\gamma = 4\sqrt{2}(1+z)/3$, where $1+z = (1-2u)^{-1/2}$ would be the red shift for photons generated at r . If the distantly observed mass accretion rate would be \dot{m}_∞ , then the impact pressure at r would be $p_i = (1+z)\dot{m}_\infty\gamma v_r/(4\pi rH)$. For $\dot{m}_\infty \sim 10^{18}$ g/s, corresponding to Eddington limit conditions for a $7 M_\odot$ GBHC, and $H = 0.0036r$, impact pressure is, $p_i \sim 5 \times 10^{16}(1+z)^2(2R_g/r)^2(6R_g/r - 1)^{3/2}$ erg/cm³. For comparison, the magnetic pressure is $(1+z)^2 B_\infty^2/8\pi$. Assuming a dipole field with average magnetic moment of 4×10^{29} gauss cm³ from Table 1, the magnetic pressure is $\sim 10^{20}(1+z)^2(2R_g/r)^6$ erg/cm³. There are no circumstances for which the impact pressure is as large as the magnetic pressure for $2R_g < r < 6R_g$. Thus we conclude that another weighty boundary layer must form inside r_{ms} in order to push the magnetosphere inward. The inner radius of the disk is determined by the rate at which the magnetic field can strip matter and angular momentum from the disk. This occurs in a boundary layer of some thickness, δr , that is only a few times the disk thickness. (See Appendix D)

Other than the presence of a transition boundary layer on the magnetopause, the nature of the flow and spectral formation inside r_c is a research topic. Both the short distance from r_c to r_{ms} and the magnetopause topology should help to maintain a disk-like flow to r_{ms} . Radial acceleration inside r_{ms} should also help to maintain a thin structure. These flows are depicted in Figure 1. As discussed in Section 4, we expect the flow into the MECO to produce a distantly observed soft thermal component, part of which is strongly bulk Comptonized.

Although many mechanisms have been proposed for the high frequency quasi-periodic oscillations (QPO) of x-ray luminosity, they often require conditions that are incom-

TABLE 1
^aCALCULATED AND OBSERVED QUIESCENT LUMINOSITIES

Object	m M _⊙	L_{min} 10 ³⁶ erg/s	L_c 10 ³⁶ erg/s	μ_{27} Gauss cm ³	ν_{obs} Hz obs.	ν_{calc} Hz calc.	log (L_q) erg/s obs.	log (L_q) erg/s calc.
NS								
Aql X-1	1.4	1.2	0.4	0.47	549	658	32.6	32.5
4U 1608-52	1.4	10	2.9	1.0	619	534	33.3	33.4
Sax J1808.4-3658	1.4	^b 0.8	0.2	0.53	401	426	31.8-32.2	32
Cen X-4	1.4	4.4	1.1	1.1		430	32.4	32.8
KS 1731-26	1.4		1.8	1.0	524		^c 32.8	33.1
XTE J1751-305	1.4		3.5	1.9	435		<34.3	33.7
XTE J0929-314	1.4		4.9	8.5	185			33.1
4U 1916-053	1.4	~14	3.2	3.7	270	370		33.0
4U1705-44	1.4	26	7	2.5		470		33.7
4U 1730-335	1.4	10		2.5	307			32.9
GRO J1744-28	1.4		18	13000	2.14			31.5
Cir X-1	1.4	300	14	170		35		32.8
GBHC								
GRS 1124-68	5	240	6.6	720		16	< 32.4	32.7
GS 2023+338	7	1000	48	470		46	33.7	34
XTE J1550-564	7	^d 90	4.1	150		45	32.8	32.2
GS 2000+25	7		0.15	160		14	30.4	30.5
GRO J1655-40	7	31	1.0	250		19	31.3	31.7
A0620-00	4.9	4.5	0.14	50		26	30.5	30.2
Cygnus X-1	10		30	1260		23		33
GRS 1915+105	7		12	130	^e 67			33
XTE J1118+480	7		1.2	1000		8		31.5
LMC X-3	7	600	7	860		16		33

^aNew table entries in bold font are described in Appendix E.

Equations used for calculations of spins, magnetic moments and L_q are in Appendix D.

Other tabular entries and supporting data are in Robertson & Leiter (2002)

^b2.5 kpc, ^c(Burderi et al. 2002), ^dd = 4 kpc

^eGRS 1915+105 Q ≈ 20 QPO was stable for six months and a factor of five luminosity change.

patible with thin, viscous Keplerian disks. Several models have requirements for lumpy flows, elliptical inner disk boundaries, orbits out of the disk plane or conditions that should produce little radiated power. In a conventional thin disk, the vertical oscillation frequency, which is approximately the same as the Keplerian frequency of the inner viscous disk radius should generate ample power. Accreting plasma should periodically wind the poloidal MECO magnetic field into toroidal configurations until the field lines break and reconnect across the disk. Field reconnection across the disk should produce high frequency oscillations that couple to the vertical oscillations. There would be an automatic association of high frequency QPO with magnetospherically driven power law emissions, as is observed. Mass ejection in low state jets might be related to the heating of plasma via the field breakage mechanism, in addition to natural buoyancy of a plasma magnetic torus in a poloidal external field.

It seems possible that toroidal winding of field lines at the magnetopause, breakage and reconnection might continue in high states inside r_{ms} . If so, there might be QPO that could be identified as signatures of the MECO magnetosphere. If they occur deep within the magnetosphere, they might be at locally very high frequencies, and be observed distantly red shifted as very low frequencies. As shown in Appendix C, the ‘Keplerian’ frequencies in the plunging region inside r_{ms} are given by $\nu = 1.18 \times 10^5 u^2 (1 - 2u)/m$ Hz. A maximum frequency of 437 Hz would occur for $m=10$ at the photon orbit. Of more interest, however are frequencies for $u \approx 1/2$, for which $\nu = 2950/(m(1+z)^2)$ Hz. For $1+z = 10, m = 10$; conditions that might apply to the photosphere region, $\nu \sim 3$ Hz could be produced.

Even if QPO are not produced inside r_{ms} or inside the photon sphere for GBHC, there is an interesting scale mismatch that might allow them to occur for AGN. Although the magnetic moments of AGN scale inversely with mass, the velocity of plasma inside r_{ms} does not. Thus the energy density of disk plasma inside r_{ms} will be relatively larger than magnetic field energy densities for AGN accretion disks. When field energy density is larger than kinetic energy density of matter, the field pushes matter around. When the reverse is true, the matter drags the field along. Thus toroidal winding of the field at the magnetopause could fail to occur for GBHC, but might easily do so for AGN. If the process is related to mass ejection, then very energetic jets with Lorentz factors $\gamma \sim (1+z)$ might arise from within r_{ms} for AGN. A field line breakage model of ‘smoke ring’ like mass ejection from deep within r_{ms} has been developed by Chou & Tajima (1999). In their calculations, a pressure of unspecified origin was needed to stop the flow outside r_{schw} and a poloidal magnetic field, also of unspecified origin was required. MECO provide the necessary ingredients in the form of the intrinsic MECO magnetic field. The Chou & Tajima mechanism is apparently not active inside r_{ms} for GBHC, as their jet emissions appear to be associated with the low/hard state (Pooley & Fender 2002).

Finally, some of the rich oscillatory behavior of GRS 1915+105 may be readily explained by the interaction of the inner disk and the central MECO. The objects in Table 1 have co-rotation radii of order $10R_{schw}$, which brings the low state inner disk radius in close to the central ob-

ject. A low state MECO, balanced near co-rotation would need only a small increase of mass flow rate to permit mass to flow on to the central MECO. This would produce more than 20X additional luminosity and enough radiation pressure to blow the inner disk back beyond r_c and load its mass onto the magnetic field lines where it is ejected. This also explains the association of jet outflows with the oscillatory states. Belloni et al. (1997) have shown that after ejection of the inner disk, it then refills on a viscous time scale until the process repeats. Thus one of the most enigmatic GBHC might be understood as a relaxation oscillator, for which the frequency is set by a critical mass accretion rate.

6. CONCLUSIONS

We have shown that the geodesics of physical matter would become null, in violation of the POE, if trapped surfaces of infinite red shift exist (e.g., Equations 1 - 3 and Appendix C). An enormous body of physics scholarship developed primarily over the last half century has been built on the assumption that trapped surfaces exist. Misner, Thorne & Wheeler (1973), for example in Sec. 34.6 clearly state that this is an assumption and that it underlies the well-known singularity theorems of Hawking and Penrose. In contrast, we have asserted the ‘no trapped surface condition’ and found new, quasi-stable, high red shift MECO solutions of the Einstein field equations. The physical mechanism of stability is an Eddington balance maintained by the distributed photon generation of an equipartition magnetic field. This field also serves to confine the pair plasma of the outer layers of the MECO and the MECO pair atmosphere. Red shifts of $z \sim 10^8$ have been found to be necessary for compatibility with our previously found magnetic moments for GBHC.

Strong magnetic fields are the robust hallmarks of MECO. Their existence in GBHC and AGN is implied by their synchrotron radiations, and is also clearly shown by the correlated data in Table 1. The spectral state switch is the signature of the magnetic field in its interaction with an accretion disk. Our work, as well as that of others, has shown that the magnetic propeller effect is the mechanism of the spectral state switch. These changes of spectral characteristics and luminosity have been observed for AGN, GBHC and NS, for which there are independent, confirming measurements of spin that show the switch to be taking place with the inner radius of the accretion disk at the co-rotation location. For the NS, the agreement between calculated and observed quiescent luminosities confirms that the quiescent power law emissions are magnetic dipole radiation. Since magnetic dipole radiation is proportional to the fourth power of the spin, the lower quiescent luminosities of the GBHC are simply a result of their slower spins.

It may be possible to observe MECO in several other ways. Firstly, as we have shown, for a red shift of $z \sim 10^8$, the quiescent luminosity of a GBHC MECO would be $\sim 10^{31}$ erg/s with $T_\infty \sim 0.01$ keV. This thermal peak might be observable for nearby or high galactic latitude GBHC, such as A0620-00 or XTE J1118+480. Secondly, at moderate luminosities $L \sim 10^{36} - 10^{37}$ erg/s but in a high state at least slightly above L_c , a central MECO would be a bright, small central object that might be sharply eclipsed in deep dipping sources. A MECO should

stand out as a bright point source. A conclusive demonstration that the most of the soft luminosity of a high state GBHC is distributed over a large radius would be inconsistent with MECO or any other GBHC model entailing a central bright source. Thirdly, a pair plasma atmosphere in an equipartition magnetic field should be virtually transparent to photon polarizations perpendicular to the magnetic field lines. The x-rays from the central MECO should exhibit some polarization that might be detectable, though this is far from certain since the distantly observed emissions could originate from nearly any point on the photosphere. Fourthly, an equipartition magnetic moment in a slowly rotating MECO might not necessarily be aligned parallel to the spin axis. It might be possible to observe pulsar oscillations under some circumstances. This possibility should be tempered with the observation that most NS in LMXB exhibit no pulsations in either x-ray or radio bands despite their magnetic moments. Finally, MECO presumably would not be found only in binary systems. If they are the offspring of massive star supernovae, they should be found all over the galaxy. If we have correctly estimated their quiescent temperatures, isolated MECO would be weak, possibly polarized, EUV sources.

The MECO model, based on the firm ground of the Principle of Equivalence, represents a paradigm shift for astrophysics. As a unified model, it provides a natural explanation of the ‘ultrasoft’ high state thermal spectrum.

The high state power law emissions are due to bulk compaction of photons from the MECO photosphere as their spiral trajectories take most of them across the flow inside r_{ms} . The weaker power law emissions of NS are a result of less source compactness and fewer photons from the surface having trajectories that cross the disk. The MECO model includes a magnetic moment and a mechanism for the spectral state switch. It accounts for low state jets and equatorial outflows as magnetic propeller effects. Its empty inner disk in quiescence is consistent with the disk instability model with its viscous timescale for the interval between optical and x-ray brightening during outbursts. The accretion disk is dominated by gas pressure in all states. The MECO model accounts for the power law portions of the quiescent luminosity as magnetospheric spin-down emissions. As we have shown in Table 1, the spectral state switch, spin, magnetic moment and quiescent luminosity are firmly linked. The low state jets and outflows, with their synchrotron emissions, are obviously linked to strong magnetic fields. It is generally accepted that an intrinsic magnetic moment in the central object is completely consistent with the behaviour of NS. The spectral, timing and synchrotron emission similarities of NS and GBHC are also well known (e.g. Tanaka & Shibazaki 1996, van der Klis 1994). It strains credulity to think that GBHC can duplicate these richly complex and obviously magnetic phenomena with just an event horizon and a tricky disk.

REFERENCES

- Abramowicz, M., Kluzniak, W. & Lasota, J-P, 2002 A&A submitted astro-ph/0207270
 Barret, D. & Olive, J-F., 2002 ApJ accepted astro-ph/0205184
 Belloni, T., Mendez, M., King, A., van der Klis, M. & van Paradijs, J. 1997 ApJ 488, L109
 Bhattacharya D., & Srinivasan, G., 1995 in ‘X-Ray Binaries’, eds W. Lewin, J. van Paradijs & E. van den Heuvel, Cambridge Univ. Press
 Boyd, P. et al. 2000 ApJ 542, L127
 Burderi, L., et al. 2002 ApJ 574, 930
 Campana, S. et al., 2001 ApJ in press astro-ph/0107326
 Campana, S. et al., 1998 A&A Rev. 8, 279
 Chou & Tajima 1999 ApJ 513, 401
 Church, M.J. 2001 in Advances in Space Research, 33rd Cospar Scientific Assembly, Warsaw, Poland July 2000 astro-ph/0012411
 Church, M. & Balucinska-Church, M. 2001 A&A 369, 915 astro-ph/0102019
 Corbel, S. & Fender, R. 2002 ApJ 573, L35
 Cui, W. 1997 ApJ 482, L163
 Done, C. & Życki, P. 1999 MNRAS 305, 457
 Galloway, D., Chakrabarty, D., Morgan, E., & Remillard, R. 2002 ApJ 576, L000 (Sept. 10)
 Garcia, M. et al. 2001 ApJ 553, L47
 Gliozzi, M., Bodo, G. & Ghisellini, G. 1999 MNRAS 303, L37
 Gnedin, Y., Silantev, N. & Titarchuk, L. astro-ph/0207640
 Hernandez Jr., W.C. & Misner, C.W., 1966 ApJ. 143, 452
 Ilarianov, A. & Sunyaev, R. 1975 A&A 39, 185
 Kato, Y., et al. 2001 in Advances in Space Research, 33rd Cospar Scientific Assembly, Warsaw, Poland July 2000 astro-ph/0104130
 Kippenhahn, R. & Weigert, A. 1990 ‘Stellar Structure and Evolution’ Springer-Verlag, Berlin Heidelberg New York
 Landau, L. & Lifshitz, E. 1958 ‘Statistical Physics’, Pergamon Press LTD, London
 Lindquist, R. W., Schwartz, R. A. & Misner, C. W. 1965 Phys. Rev., 137B, 1364.
 Lindquist, R. W., 1966 Annals of Physics, 37, 487
 Markoff, S., Falcke H., & Fender, R. 2001 A&AL 372, 25
 Markwardt, C., et al. 2002 ApJL submitted, astro-ph/0206491
 McClintock, J. et al., 2001 ApJ 556, 42
 Miller, J. et al., 2002 astro-ph/0208166
 Misner, C. W. 1965 Phys. Rev., 137B, 1360
 Misner, C., Thorne, K. & Wheeler, J. 1973 ‘Gravitation’, Freeman, San Francisco, California
 Mitra, A. 2000 Found. Phys. Lett. 13, 543
 Mitra, A., 2002 Found. Phys. Lett. (accepted for publication), (astro-ph/0207056)
 Muno, M., Remillard, R. & Chakrabarty, D. 2002 ApJ 568, L35
 Narayan, R., Garcia, M., McClintock, J., 1997 ApJ. 478, L79
 Orosz, J., Remillard, R., Bailyn, C. & McClintock, J. 1997 ApJ 478, L83
 Paragi, Z., et al. astro-ph/0208125
 Pelletier, G. & Marcowith, A., 1998 ApJ 502, 598
 Possenti, A., Cerutti, R., Colpi, M., & Mereghetti, S. 2002 A&A 387, 993
 Robertson, S. & Leiter, D. 2002 ApJ, 565, 447 (astro-ph/0102381)
 Shapiro, S. & Teukolsky, S. 1983 in ‘Black Holes, White Dwarfs & Neutron Stars’, John Wiley & Sons, Inc., New York
 Soria, R., Page, M. & Wu, K. 2002 astro-ph/0202015
 Spruit, H. & Taam, R. 1990 A&A 229, 475
 Stella, L., White, N. & Rosner, R. 1986 ApJ 308, 669
 Strohmayer, T. in Advances in Space Research, 33rd Cospar Scientific Assembly, Warsaw, Poland July 2000
 Tanaka, Y. & Lewin, W., 1995 in ‘Black-hole binaries’ in X-ray Binaries ed. W. Lewin, J. van Paradijs & E. van den Heuvel (Cambridge: Cambridge Univ. Press)
 Tanaka, Y. & Shibazaki, N., 1996 ARA&A, 34, 607
 Vadawale, S., Rao, A. & Chakrabarti, S. 2001 A&A 372, 793V
 van der Klis, M. 1994 ApJS 92, 511
 Wheeler, J. & Ciufolini, I., 1995 in ‘Gravitation And Inertia’ Princeton Univ. Press, 41 William St., Princeton, New Jersey
 White, N. & Marshall, F. 1984, ApJ. 281, 354
 Wilson, C. & Done, C. 2001 MNRAS 325, 167
 Zhang, W., Yu, W. & Zhang, S. 1998 ApJ 494, L71
 Życki, P., Done, C. and Smith, D. 1997a in AIP Conf. Proc. 431, Accretion Processes in Astrophysical Systems: Some Like It Hot, Ed. S. S. Holt & T. R. Kallman (New York, AIP), 319
 Życki, P., Done, C. and Smith 1997b ApJ 488, L113

APPENDIX

A. Eddington Limited Collapse for MECO

Let us assume an energy momentum tensor which involves matter, pressure, and radiation

$$T_{\mu}^{\nu} = (\rho + P/c^2)u_{\mu}u^{\nu} - P\delta_{\mu}^{\nu} + E_{\mu}^{\nu} \quad (1)$$

where $u^{\mu} = (u^0, 0)$ in the interior where co-moving coordinates are used and $E_{\mu}^{\nu} = qk_{\mu}k^{\nu}$ is the radiation part of the EM tensor in geometric optics limit, for which $k_{\mu}k^{\mu} = 0$. In interior co-moving coordinates

$$ds^2 = A^2c^2dt^2 - B^2dR^2 - R(r, t)^2(d\theta^2 + \sin^2\theta d\phi^2) \quad (2)$$

and in the exterior radiating metric:

$$ds^2 = a^2c^2dt_r^2 + 2bcdt_r dR - R(r, t_r)^2(d\theta^2 + \sin^2\theta d\phi^2) \quad (3)$$

where $dt_r = dt - R/c$ is the retarded observer time.

Now in the interior co-moving coordinates, the luminosity of radiation is $L = 4\pi R^2 qc$, $q = E_{\mu}^{\nu} = E_0^0 c^2$ is the energy density of radiation, $\Gamma = dR/dl$, $U = dR/d\tau$ and

$$\Gamma^2 = 1 - \frac{R_{schw}}{R} + \left(\frac{U}{c}\right)^2 \quad (4)$$

From the boundary condition on the time like collapsing surface $R_s = R_s(r, t_r)$ separating the interior metric from the exterior metric, and the POE, we find that the proper time of the collapsing surface is given by

$$d\tau_s = \frac{dt_r}{1 + z_s} = dt_r(\Gamma_s + U_s/c) > 0 \quad (5)$$

To analyze the physical gravitational collapse process one proceeds to solve the Einstein equations for the interior co-moving metric with boundary conditions which connect the interior metric to the exterior metric at the collapsing surface. When this is done, as described by the Einstein equations in the co-moving metric (Hernandez Jr. & Misner, 1966, Lindquist, Schwartz & Misner 1965, Misner 1965, Lindquist, 1966), we find that among the various equations associated with the collapse process there are three proper time differential equations which control the physical properties of a compact collapsing and radiating physical surface. When evaluated on the physical surface these equations are given by:

$$\frac{dU_s}{d\tau} = \left(\frac{\Gamma}{\rho + P/c^2}\right)_s \left(-\frac{\partial P}{\partial R}\right)_s - \left(\frac{G(M + 4\pi R^3(P + q)/c^2)}{R^2}\right)_s \quad (6)$$

$$\frac{dM_s}{d\tau} = -(4\pi R^2 P c \frac{U}{c})_s - (L(\frac{U}{c} + \Gamma))_s \quad (7)$$

$$\frac{d\Gamma_s}{d\tau} = \frac{G}{c^4} \left(\frac{L}{R}\right)_s + \frac{U_s}{c^2} \left(\frac{\Gamma}{\rho + P/c^2}\right)_s \left(-\frac{\partial P}{\partial R}\right)_s \quad (8)$$

Now we have seen from Section 2 that in all frames of reference the POE requires that $1/(1 + z_s) > 0$ must hold in the context of the time-like gravitational collapse of physical matter. This POE therefore implies that a surface of infinite red-shift cannot be dynamically formed by the time-like collapse of physical matter. Since the POE dynamic condition that $1/(1 + z_s) > 0$ holds for the time-like motion of physical matter in all frames of reference, it is also true in the context of the co-moving frame of reference for the equations of motion of the gravitationally collapsing surface defined by equations (6 - 8). Hence the Principle of Equivalence requires that equations (6 - 8) must be dynamically constrained to obey

$$\frac{1}{1 + z_s} = \Gamma_s + \frac{U_s}{c} = \left(1 - \frac{R_{schw}}{R} + \frac{U_s^2}{c^2}\right)^{1/2} + \frac{U_s}{c} > 0 \quad (9)$$

Solving this equation for the quantity R_{schw}/R we find this requires that the ‘no trapped surface condition’

$$\frac{R_{schw}}{R_s} < 1 \quad (10)$$

must hold in the equation of motion for physical matter.

It follows that the POE dynamically requires, in equations of motion for physical matter, that the ‘no trapped surface condition’, $R_{schw}/R_s < 1$ must be maintained by the physical forces which act during the collapse process. Hence we conclude that the Principle of Equivalence requires that the physical processes involved in the gravitational collapse of a physical plasma must allow it to heat up and radiate so as to allow a high red shift Eddington limited secular equilibrium to form in a manner which allows $R_{schw}/R_s < 1$ to be maintained. For a physical plasma undergoing a spherically symmetric gravitational collapse, this implies that a Magnetospheric Eternally Collapsing Object (MECO)

can dynamically form as a high red shift Eddington limited secular equilibrium object, where both $dU_s/d\tau = 0$ and $U_s(\tau_{edd}) = 0$ hold for the time-like motion of the surface layer after the proper time τ_{edd} . At this time the invariant surface radius is $R_s(\tau_{edd}) = R_{s,Edd} > R(\tau_{edd})_{schw}$ whose large but finite value of the surface red shift is given by $(1 + z_s(\tau_{edd}))$.

Then for high red shift Eddington limited MECO equation (6) with $(U_s/c) = 0$ becomes

$$\frac{dU_s}{d\tau} = \frac{\Gamma_s}{(\rho + P/c^2)_s} \left(-\frac{\partial P}{\partial R}\right)_s - \frac{G(M_s)}{R_s^2} = 0 \quad (11)$$

Where

$$M_s = (M + 4\pi R^3(P + q)/c^2)_s \quad (12)$$

Equation (11) when integrated over a closed surface for $\tau > \tau_{edd}$ can be solved for the net outward flow of Eddington limited luminosity through the surface. Since the surface $R_s(\tau_{edd})$ obeys $R(\tau_{edd})_{schw} < R_s(\tau_{edd}) < R(\tau_{edd})_{photon}$, then $\Gamma(\tau_{edd})_s > 0$ and the photon escape cone factor $27(R(\tau_{edd})_{schw}/2R_s(\tau_{edd}))^2(1 - R(\tau_{edd})_{schw}/R_s(\tau_{edd}))$ ($\sim (27/4)(1 + z_{edd})^2$ for $R_s \sim R_{schw}$) must be taken into account in the calculation of Eddington limit luminosity.

When this is done one finds that the outflowing (but not all escaping) Eddington luminosity emitted from the surface is (see Appendix B) given by

$$L_{edd}(outflow)_s = \frac{4\pi GM(\tau)_s c(1 + z_{edd})^3}{27\kappa u_s^2} \quad (13)$$

where $u_s = GM_s/c^2 R_s$. (For simplicity, we have assumed here that the luminosity actually escapes from the MECO surface rather than after conveyance through an atmosphere and photosphere. The end result is the same for distant observers.) However the luminosity L_s which appears in equations (7-8) is actually the net luminosity, which escapes through the photon radius, and is given by $L_s = L_{edd}(escape)_s = L_{edd}(outflow) - L_{edd}(fallback) = L_{Edd,s} - L_{Edd,s}(1 - 27(R_{schw}/2R_s)^2(1 + z_{edd})^2)$ Thus in equations 7 and 8, the L_s appearing there is given by

$$L_s = L_{edd}(escape)_s = \frac{4\pi GM(\tau)_s c}{\kappa(1 + z_{edd})} \quad (14)$$

In this context from (7) we have that

$$\frac{dM_s}{d\tau} = -\frac{L_{edd}(escape)_s}{(1 + z_{edd})^2} = -\frac{4\pi GM(\tau)_s c}{\kappa c^2} = \frac{c^2}{2G} U_{schw} \quad (15)$$

which can be integrated for $\tau > \tau_{edd}$ to give

$$M_s(\tau) = M_s(\tau_{edd}) \exp((-4\pi G/\kappa c)(\tau - \tau_{edd})) \quad (16)$$

Finally, equation (8) becomes

$$\frac{d\Gamma_s}{d\tau} = \frac{G}{c^4} \frac{L_{edd,s}}{R_s(\tau_{edd})} = \frac{4\pi G}{2\Gamma_s \kappa c} \frac{R(\tau)_{schw}}{R_s(\tau_{edd})} \quad (17)$$

whose solution

$$\Gamma_s(\tau) = \frac{1}{1 + z_s(\tau)} = \left(1 - \frac{R(\tau)_{schw}}{R_s(\tau)_{edd}}\right)^{1/2} > 0 \quad (18)$$

is consistent with (4) and (9).

Hence from the above we have for the high red shift MECO solutions to the Einstein Equations that $R_s(\tau) = R_s(\tau_{edd})$, $U(\tau) = U(\tau_{edd}) = 0$ and

$$R(\tau)_{schw} = (R(\tau_{edd})_{schw}) \exp((-4\pi G/\kappa c)(\tau - \tau_{edd})) < R_s(\tau) = R_s(\tau_{edd}) \quad (19)$$

$$U(\tau)_{schw}/c = (U(\tau_{edd})_{schw}/c) \exp((-4\pi G/\kappa c)(\tau - \tau_{edd})) < U(\tau)/c = U(\tau_{edd})/c = 0 \quad (20)$$

where $U(\tau_{edd})_{schw} = -(R(\tau_{edd})_{schw} 4\pi G/\kappa c^2)$ and

$$\Gamma_s(\tau) = \left(1 - \frac{R(\tau)_{schw}}{R_s(\tau)_{edd}}\right)^{1/2} = \frac{1}{1 + z_{edd}(\tau)} = \left(1 - \frac{R(\tau_{edd})_{schw}}{R_s(\tau_{edd})} \exp((-4\pi G/\kappa c)(\tau - \tau_{edd}))\right)^{1/2} \quad (21)$$

with

$$1 + z(\tau)_{edd} = \left(1 - \frac{R(\tau_{edd})_{schw}}{R_s(\tau_{edd})} \exp((-4\pi G/\kappa c)(\tau - \tau_{edd}))\right)^{-1/2} \quad (22)$$

Hence for $1 + z(\tau_{edd}) \sim 10^8$ and proper time $\tau > \tau_{edd}$ it follows that distant observers see the MECO mass decay and red shift increase with an extremely long e-folding time of $4.5 \times 10^8(1 + z_s)$ yr; $\sim 2 \times 10^7(t_{Hubble})$.

APPENDIX

B. Relativistic Eddington Limit Formulas

From the equation 11 of Appendix A, in the Eddington limit at a surface,

$$\Gamma_{edd}\left(-\frac{\partial P}{\partial r}\right)_{edd} = (\rho + P/c^2)_s \frac{GM_s}{R_s^2} \quad (1)$$

When integrated over a closed surface for $\tau > \tau_{edd}$ equation (1) can be solved for the net outward flow of Eddington limited luminosity through the surface. Since the surface $R_s(\tau_{edd})$ obeys $R(\tau_{edd})_{schw} < R_s(\tau_{edd}) < R(\tau_{edd})_{photon}$, then $\Gamma_s(\tau_{edd}) > 0$ and the photon escape cone factor $27(R(\tau_{edd})_{schw}/2R_s(\tau_{edd}))^2(1 - R(\tau_{edd})_{schw}/R_s(\tau_{edd}))$ must be taken into account in doing the calculation. Then integrating this equation over a plasma shell of radius R_s

$$\int (4\pi R_s^2 dR_s \Gamma_{edd}\left(-\frac{\partial P}{\partial R}\right)_{edd} = \int (4\pi GM_s(\rho + \frac{P}{c^2})_s) dR \quad (2)$$

$$\Gamma_{edd} 4\pi \int R_s^2 dP_{edd} = 4\pi GM_s \int (\rho + P/c^2)_s dR \quad (3)$$

where

$$\Gamma_{edd} = 1/(1 + z_{edd}). \quad (4)$$

Associated with its high compactness and temperature, the MECO plasma evolves into an optically thick pair plasma. Hence the number of protons plus positrons will match the number of electrons in the shell. Then radiation pressure transfers momentum to the electrons and positrons, which then support the protons through coulomb interactions. Then if the number of protons per cm^2 in the shell is N_s , it follows that

$$\int (\rho + P/c^2)_s dR = m_p N_s, \quad (5)$$

where m_p is the proton rest mass. Then

$$\int 4\pi R_s^2 dP_{edd} = \kappa N_s m_p L_{edd}(escape)_s / c \quad (6)$$

Where κ is MECO opacity and $L_{edd}(escape)_s$ is the net luminosity which escapes through the photon radius (the remainder falls back into the shell). It is given by $L_{edd}(escape)_s = L_{edd}(outflow) - L_{edd}(fallback) = L_{Edd,s} - L_{Edd,s}(1 - 27(R_{schw}/2R_s)^2(1 + z_{edd})^2)$ Solving equations (2-6) we have locally that

$$L_{edd}(outflow)_s = \frac{4\pi GM_s(\tau)c(1 + z_{edd})^3}{27\kappa u_s^2} \quad (7)$$

where $u_s = GM_s/c^2 R_s$ and hence that

$$L_{edd}(escape)_s = \frac{4\pi GM_s(\tau)c}{\kappa(1 + z_{edd})} \quad (8)$$

which implies that the red shift at which the Eddington limit is established is given by

$$1 + z_{edd} = \left(\frac{L_{edd}(outflow)_s 27 u_s^2 \kappa}{4\pi GM_s}\right)^{1/3} \quad (9)$$

while the net Eddington luminosity seen at infinity is

$$L_{Edd,\infty} = \frac{L_{edd}(escape)_s}{(1 + z_{edd})^2} = \frac{4\pi GM_s c}{\kappa(1 + z)} \sim \frac{1.27 \times 10^{38} m}{1 + z} \text{ erg/s} \quad (10)$$

APPENDIX

C. Relativistic particle mechanics

A number of standard, but useful results for relativistic mechanics are recapitulated here. All are based upon the energy-momentum four-vector for a free particle in the Schwarzschild geometry of a central mass. The magnitude of this vector, given by $g^{ij}p_i p_j$, is $m_0^2 c^2$ where m_0 is the rest mass of the particle. For a particle in an equatorial trajectory ($\theta = \pi$, $p_\theta = 0$) about an object of gravitational mass M , one obtains: $g_{00} = 1/g^{00} = -1/g_{rr} = -g^{rr} = (1 - 2u)$, $g_{\phi\phi} = -r^2$, where $u = GM/c^2 r$. $p_0 = E/c$, $p^r = m_0 dr/d\tau$, $p^\phi = m_0 d\phi/d\tau$. Here E is the particle energy as judged by a distant oberver

positioned where $u = 0$. In the event $m_0 = 0$, some parameter, λ , must be used instead of the proper time of a photon to describe its trajectory. With these preliminaries, the energy-momentum equation is.

$$\frac{E^2}{(1-2u)c^2} - (1-2u)p_r^2 - \frac{p_\phi^2}{r^2} = m_0^2 c^2 \quad (1)$$

Using $p_r = -g_{rr}p^r$ and $e = E/m_0c^2$, there follows

$$\left(\frac{dr}{d\tau}\right)^2 = c^2(e^2 - (1-2u)(1+a^2u^2)) \quad (2)$$

Where $a = (cp_\phi/GMm_0)$ is a dimensionless, conserved angular momentum. For suitably small energy, bound orbits occur. Turning points for which $dr/d\tau = 0$ can be found by examining the effective potential, which consists of all terms to the right of e^2 . At minima of the effective potential we find circular orbits for which

$$a^2 = \frac{1}{u-3u^2} \quad (3)$$

$u = 1/3$ holds at the location of an unstable circular orbit for photons (see below). From which we see that if p_ϕ is non-zero there are no trajectories for particles with both mass and angular momentum that exit from within $u = 1/3$. Thus particles with both mass and angular momentum can't escape from within the photon sphere. The minimum energy required for a circular orbit would be.

$$E = m_0c^2 \frac{(1-2u)}{\sqrt{(1-3u)}} \quad (4)$$

In fact, however, there is an innermost marginally stable orbit for which the first two derivatives with respect to r or u of the effective potential vanish. This has no Newtonian physics counterpart, and yields the well-known results: $u = 1/6$, $a^2 = 12$ and $e^2 = 8/9$ for the marginally stable orbit of radius $r_{ms} = 6GM/c^2$.

For a particle beginning a radial free-fall with $a = 0$ the particle energy-momentum equation becomes

$$dr^2 = c^2 d\tau^2 (e^2 - (1-2u))^{1/2} \quad (5)$$

But since $p_0 = E/c = g_{00}p^0 = (1-2u)m_0cdt/d\tau$, we find

$$d\tau = dt(1-2u)/e \quad (6)$$

Therefore, on the particle trajectory r and t are related by

$$dr^2/(1-2u) = c^2 dt^2 (1-2u)(1-(1-2u)/e^2) \quad (7)$$

Substituting this into the radial Schwarzschild metric equation

$$ds^2 = (1-2u)c^2 dt^2 - dr^2/(1-2u) \quad (8)$$

yields

$$ds^2 = (1-2u)c^2 dt^2 - (1-2u)c^2 dt^2 (1-(1-2u)/e^2) = (1-2u)^2 c^2 dt^2 / e^2 \quad (9)$$

Unless one is prepared to argue that the infinitesimal dt can approach infinity, this result makes it quite clear that the time-like geodesic of a radially falling particle would become null if $u = 1/2$, in violation of the Principle of Equivalence. Of course, this result was obvious earlier in Equation 6. Further, a stationary observer positioned at coordinate r , would observe the particle to have radial speed

$$V_r = \frac{\sqrt{g_{rr}}dr}{\sqrt{g_{00}}dt} = c\left(1 - \frac{(1-2u)}{e^2}\right)^{1/2} \quad (10)$$

which would yield $V_r = c$ as $u = 1/2$. For $u < 1/2$, the Lorentz factor is $\gamma = (1 - V_r^2/c^2)^{-1/2} = (1+z)e$, where $(1+z) = (1-2u)^{-1/2}$ would be the red shift for photons emitted from r .

For a particle beginning a spiral descent from r_{ms} with $e = \sqrt{8/9}$, there follows:

$$\left(\frac{dr}{d\tau}\right)^2 = c^2 \frac{(6u-1)^3}{9} \quad (11)$$

If observed by a stationary observer located at coordinate r , it would be observed to move with radial speed

$$V_r = \frac{\sqrt{-g_{rr}}dr}{\sqrt{g_{00}}dt} = \frac{\sqrt{2}c(6u-1)^{3/2}}{4} \quad (12)$$

Again, V_r approaches c as u approaches $1/2$. A distant observer would find the angular frequency of the spiral motion to be

$$\frac{1}{2\pi} \frac{d\phi}{dt} = \sqrt{9 \times 12/8} (c^3/GM) u^2 (1-2u)/2\pi \sim 1.18 \times 10^5 u^2 (1-2u)/m \quad \text{Hz} \quad (13)$$

For a $10 M_\odot$ GBHC ($m = 10$), this has a maximum of 437 Hz and some interesting possibilities for generating many QPO frequencies, both high and low. For red shifts such that $u \approx 1/2$, the spiral frequency is $2950/(1+z)^2$ Hz.

Photon Trajectories:

The energy-momentum equation for a particle with $m_0 = 0$ can be rearranged as:

$$(1-2u)^2 \left(\frac{p_r GM}{p_\phi c^2} \right)^2 = \left(\frac{du}{d\phi} \right)^2 = \left(\frac{GME}{p_\phi c^3} \right)^2 - u^2 (1-2u) \quad (14)$$

The right member has a maximum value of $1/27$ for $u = 1/3$. There is an unstable orbit with $du/d\phi = 0$ for $u = 1/3$. To simply have $du/d\phi$ be real requires $p_\phi c^3/GME < \sqrt{27}$. But $E = (1+z)pc$, where p is the entire momentum of the photon, and $1+z = (1-2u)^{-1/2}$ its red shift if it escapes to be observed at a large distance. Its azimuthal momentum component will be p_ϕ/r . Thus its escape cone is defined by:

$$\left(\frac{p_\phi}{rp} \right)^2 < 27u^2 (1-2u) \quad (15)$$

APPENDIX

D. Magnetosphere - Disk Interaction

The torque per unit volume of plasma in the disk threaded by magnetic field is given by $r \frac{B_z}{4\pi} \frac{\partial B_\phi}{\partial z} \sim r \frac{B_z B_\phi}{4\pi H}$, where H is the disk half thickness. Thus the rate at which angular momentum would be removed from the disk would be

$$\dot{m}(v_K - 2\pi\nu_s r) = r \frac{B_z B_\phi}{4\pi H} (4\pi H \delta r). \quad (1)$$

The conventional expression for the magnetosphere radius can be obtained with two additional assumptions: (i) that the field is fundamentally a dipole field that is reshaped by the surface currents of the inner disk and (ii) that $B_\phi = \lambda B_z (1 - 2\pi\nu_s r/v_k)$, where λ is a dimensionless constant of order unity. This form accounts for the obvious facts that B_ϕ should go to zero at r_c , change sign there and grow in magnitude at greater distances from r_c . In fact, however, we should note that we are only describing an average B_ϕ here, because it is possible that the field lines become overly stretched by the mismatch between magnetospheric and Keplerian disk speeds, then break and reconnect across the disk. This type of behavior leads to high frequency oscillations and has been described in numerical simulations (Kato 2000). With these assumptions we obtain

$$r = \left(\frac{\lambda \delta r}{r} \right)^{2/7} \left(\frac{\mu^4}{GM\dot{m}^2} \right)^{1/7} \quad (2)$$

In order to estimate $\delta r/r$, we choose an object for which few would quibble about it being magnetic; namely an atoll class NS. The rate of spin is typically 400 - 500 Hz, the co-rotation radius is ~ 26 km, and the maximum luminosity for the low state is $\sim 2 \times 10^{36} = GM\dot{m}/2r$ erg/s, from which $\dot{m} = 5.5 \times 10^{16}$ g/s, for $M = 1.4M_\odot$. For a magnetic moment of $\sim 10^{27}$ gauss cm³, we find that $(\frac{\lambda \delta r}{r})^{2/7} \sim 0.3$. Thus if $\lambda \sim 1$, then $\delta r/r \sim 0.013$; i.e., the boundary region is suitably small, though larger than the scale height of the trailing disk. In this small region the flow changes from co-rotation with the magnetosphere to Keplerian. When its inner radius is inside r_c , its weight is not entirely supported by centrifugal forces and it provides the 'dead-weight' against the magnetopause.

The equations needed for analysis of the data in Table 1 were developed in previous work (Robertson & Leiter 2002). Using units of 10^{27} gauss cm³ for magnetic moments, 100 Hz for spin, 10^6 cm for radii, 10^{15} g/s for accretion rates, solar mass units, $\lambda \delta r/r = 0.013$ and otherwise obvious notation we found the magnetosphere radius to be:

$$r_m = 8 \times 10^6 \left(\frac{\mu_{27}^4}{m\dot{m}_{15}^2} \right)^{1/7} \quad \text{cm} \quad (3)$$

A co-rotation radius of:

$$r_c = 7 \times 10^6 \left(\frac{m}{\nu_2^2} \right)^{1/3} \quad \text{cm} \quad (4)$$

The low state luminosity at the co-rotation radius:

$$L_c = 1.5 \times 10^{34} \mu_{27}^2 \nu_2^3 m^{-1} \quad \text{erg/s} \quad (5)$$

High state luminosity for accretion reaching the central object:

$$L_s = \xi \dot{m} c^2 = 1.4 \times 10^{36} \xi \mu_{27}^2 \nu_2^{7/3} m^{-5/3} \quad \text{erg/s} \quad (6)$$

Where $\xi \sim 1$ for MECO and $\xi = 0.14$ for NS is the efficiency of accretion to the central surface. We have recalculated the quiescent luminosities in the soft x-ray band from 0.5 - 10 keV using the correlations of Possenti et al. (2001) with spin-down energy loss rate as:

$$L_q = \beta \dot{E} = \beta 4\pi^2 I \nu \dot{\nu} \quad (7)$$

where I is the moment of inertia of the star, ν its rate of spin and β a multiplier that can be determined from the new $\dot{E} - L_q$ correlation for given \dot{E} ; i.e., known spin and magnetic moment. (In previous work we had used $\beta = 10^{-3}$ for all objects.) We assume that the luminosity is that of a spinning magnetic dipole for which $\dot{E} = 32\pi^4 \mu^2 \nu^4 / 3c^3$, (Bhattacharya & Srinivasan 1995) where μ is the magnetic moment. Thus the quiescent x-ray luminosity would then be given by :

$$L_q = \beta \times \frac{32\pi^4 \mu^2 \nu^4}{3c^3} = 3.8 \times 10^{33} \beta \mu_{27}^2 \nu_2^4 \quad \text{erg/s} \quad (8)$$

As the magnetic moment, μ_{27} , enters each of the luminosity equations it can be eliminated from ratios of these luminosities, leaving relations involving only masses and spins. For known masses, the ratios then yield the spins. Alternatively, if the spin is known from burst oscillations, pulses or spectral fit determinations of r_c , one only needs one measured luminosity to enable calculation of the remaining μ_{27} and L_q . For most GBHC, we found it to be necessary to estimate the co-rotation radius from multicolor disk fits to the thermal component of low state spectra. The reason for this is that the luminosities are seldom available across the whole spectral hardening transition of GBHC. For GBHC, it is a common finding that the low state inner disk radius is much larger than that of the marginally stable orbit (e.g. Markoff, Falcke & Fender 2001, Życki, Done & Smith 1997a,b 1998, Done & Życki 1999, Wilson & Done 2001). The presence of a magnetosphere is an obvious explanation. Given an inner disk radius at the spectral state transition, the GBHC spin frequency follows from the Kepler relation $2\pi\nu_s = \sqrt{GM/r^3}$.

APPENDIX

E. Observational Data

The third accreting millisecond pulsar, **XTE J0929-314** has been found (Galloway et al. 2002) with $\nu_s = 1/P = 185$ Hz and period derivative $\dot{P} = 2.69 \times 10^{-18}$, from which the magnetic field (calculated as $3.2 \times \sqrt{P\dot{P}}$) is 3.9×10^9 gauss. This is typical of a Z source. Assuming a NS radius of 13 km, the magnetic moment is $BR^3 = 8.5 \times 10^{27}$ gauss cm³. The calculated low state limit co-rotation luminosity is $L_c = 4.9 \times 10^{36}$ erg/s. Approximately 40% of this would be the luminosity in the (2 - 10 keV) band. This yields an expected flux of 2×10^{-10} erg/cm²/s for a distance of 9 kpc. This corresponds to the knee of the published light curve where the luminosity begins a rapid decline as the propeller becomes active. Similar breaking behavior has been seen in Sax J1808.4-3659 and GRO J1655-40 at propeller onset. The predicted 0.5-10 keV band luminosity is $L_q = 1.3 \times 10^{33}$ erg/s.

The second accreting millisecond pulsar **XTE J1751-305** was found with a spin of 435 Hz. (Markwardt et al. 2002) Its spectrum has been analyzed (Miller et al. 2002). We find a hard state luminosity of 3.5×10^{36} erg/s ($d = 8$ kpc) at the start of the rapid decline which is characteristic of the onset of the propeller effect. We take this as an estimate of L_c . From this we estimate a magnetic moment of 1.9×10^{27} gauss cm³ and a quiescent luminosity of 5×10^{33} erg/s. An upper limit on quiescent luminosity of 1.8×10^{34} erg/s can be set by the detections of the source in late April 2002, as reported by Markwardt et al. (2002).

The accreting x-ray pulsar, **GRO J1744-28** has long been cited for exhibiting a propeller effect. Cui (1997) has given its spin frequency as 2.14 Hz and a low state limit luminosity as $L_c = 1.8 \times 10^{37}$ erg/s (2 - 60 keV.), for a distance of 8 kpc. These imply a magnetic moment of 1.3×10^{31} gauss cm³ and a magnetic field of $B = 5.9 \times 10^{12}$ gauss for a 13 km radius. Its spin-down energy loss rate should be $\dot{E} = 1.4 \times 10^{35}$ erg/s and its quiescent luminosity, $L_q = 3 \times 10^{31}$ erg/s. Due to its slow spin, GRO J1744-28 has a large co-rotation radius of 280 km. A mass accretion rate of $\dot{m} = 5.4 \times 10^{18}$ g/s is needed to reach L_c . Larger accretion rates are needed to reach the star surface, but such rates distributed over the surface would produce luminosity in excess of the Eddington limit. The fact that the magnetic field is strong enough to funnel a super-Eddington flow to the poles is the likely reason for the type II bursting behavior sometimes seen for this source. In addition to its historical illustration of a propeller effect, this source exemplifies the inverse correlation of spin and magnetic field strength in accreting sources. It requires a weak field to let an accretion disk get close enough to spin up the central object. For this reason we expect Z sources with their stronger B fields to generally spin more slowly than atolls.

The accreting pulsar, **4U0115+63**, with a spin of 0.276 Hz and a magnetic field, derived from its period derivative, of 1.3×10^{12} gauss (yielding $\mu = 2.9 \times 10^{30}$ gauss cm³ for a 13 km radius) has been shown (Campana et al. 2002) to exhibit a magnetic propeller effect with a huge luminosity interval from $L_c = 1.8 \times 10^{33}$ erg/s to $L_{min} = 9.6 \times 10^{35}$ erg/s. L_c held steady precisely at the calculated level for a lengthy period before luminosity began increasing. Due to the slow spin of this star, its quiescent luminosity, if ever observed, will be just that emanating from the surface. Its spin-down luminosity will be much too low to be observed.

The atoll source **4U1705-44** has been the subject of a recent study (Barret & Olive 2002) in which a Z track has been displayed in a color-color diagram. Observations labeled as 01 and 06 mark the end points of a spectral state transition for which the luminosity ratio $L_{min}/L_c = 25.6 \times 10^{36}/6.9 \times 10^{36} = 3.7$ can be found from their Table 2. These yield $\nu = 470$ Hz and a magnetic moment of $\mu = 2.5 \times 10^{27}$ gauss cm³. The spin-down energy loss rate is 1.2×10^{37} erg/s and the 0.5 - 10 keV quiescent luminosity is estimated to be about 5×10^{33} erg/s. At the apex of the Z track (observation 12),

the luminosity was 2.4×10^{37} erg/s (for a distance of 7.4 kpc.); i.e., essentially the same as L_{min} . Although 4U1705-44 has long been classified as an atoll source, it is not surprising that it displayed the Z track in this outburst as its 0.1 - 200 keV luminosity reached 50% of the Eddington limit.

Considerable attention was paid to reports of a truncated accretion disk for the GBHC, **XTE J1118+480** (McClintock et al 2001) because of the extreme interest in advective accretion flow (ADAF) models for GBHC (Narayan, Garcia & McClintock 1997). McClintock et al, fit the low state spectrum to a disk blackbody plus power law model and found that the disk inner radius would be about $35R_{schw}$, or 720 km for $7 M_{\odot}$. Using this as an estimate of the co-rotation radius we find the spin to be 8 Hz. The the corresponding low state luminosity of 1.2×10^{36} erg/s (for $d = 1.8$ kpc) lets us find a magnetic moment of 10^{30} gauss cm^3 . The calculated spin-down energy loss rate is 1.5×10^{35} erg/s and the quiescent luminosity would be about 3×10^{31} erg/s.

A rare transition to the hard state for **LMC X-3** (Soria, Page & Wu 2002, Boyd et al. 2000) yields an estimate of the mean low state luminosity of $L_c = 7 \times 10^{36}$ erg/s and the high state luminosity in the same 2 - 10 keV band is approximately 6×10^{38} erg/s at the end of the transition to the soft state. Taking these as L_c and L_{min} permits the estimates of spin $\nu = 16$ Hz and magnetic moment $\mu = 8.6 \times 10^{29}$ gauss cm^3 , assuming $7 M_{\odot}$. From these we calculate a quiescent luminosity of 10^{33} erg/s.

APPENDIX

F. Pair Plasma Photosphere Conditions

Although we used a characteristic temperature of a pair plasma to locate the photosphere and find its temperature, essentially the same results can be obtained in a more conventional way. The photosphere condition is that (Kippenhahn & Weigert 1990):

$$n\sigma_T l = 2/3, \quad (1)$$

where n is the combined number density of electrons and positrons in equilibrium with a photon gas at temperature T , $\sigma_T = 6.65 \times 10^{-25} cm^2$ is the Thompson scattering cross section and l is a proper length over which the pair plasma makes the transition from opaque to transparent. Landau & Lifshitz (1958) show that

$$n = \frac{8\pi}{h^3} \int_0^{\infty} \frac{p^2 dp}{\exp(E/kT) + 1} \quad (2)$$

where p is the momentum of a particle, $E = \sqrt{p^2 c^2 + m_e^2 c^4}$, k is Boltzmann's constant, h is Planck's constant and m_e , the mass of an electron. For low temperatures such that $kT < m_e c^2$ this becomes:

$$n \approx 2 \left(\frac{2\pi m_e kT}{h^2} \right)^{3/2} \exp(-m_e c^2 / kT) \quad (3)$$

It must be considered that the red shift may change significantly over the length l , and that $(1 + z_p)$ will likely be orders of magnitude smaller than $(1 + z_s)$. Neglecting algebraic signs, we can differentiate equation 14 to obtain the coordinate length over which z changes significantly as:

$$\delta r = \frac{R_g \delta z}{u^2 (1+z)^3} \approx \frac{R_g}{u^2 (1+z)^2} \quad (4)$$

where we have taken $\delta z \approx (1+z)$. For values of z appropriate here we take $u = 1/2$. We estimate $l = \delta(1+z) = 4R_g/(1+z)$ and replace $(1+z)$ with T/T_{∞} . Substituting expressions for l and n into the photosphere condition and substituting for T_{∞} from equation 18 of the main text, equation 1 yields a transcendental equation for T .

For a GBHC with $z = 10^8$ and $m = 10$, the solution is $T_p = 3.3 \times 10^8 K$ and $(1 + z_p) = 2500$. Then using the radiation pressure balance condition in the pair atmosphere, we find $T_s^4 = T_p^4 (1 + z_s) / (1 + z_p)$, from which $T_s = 4.6 \times 10^9 K$. The number density of particles at the photosphere is $n = 4 \times 10^{20}$ and 10^9 times larger at the MECO surface. Nevertheless, the radiation pressure exceeds the pair particle pressure there by ten fold. This justifies our use of radiation dominated pressure in the pair atmosphere. For an AGN with $1 + z = 10^8$ and $m = 10^7$, we obtain photosphere and surface temperatures of $2 \times 10^8 K$ and $1.4 \times 10^9 K$, respectively, and $(1 + z_p) = 50000$. We note that the steep temperature dependence of the pair density would have allowed us to find the same photosphere temperature within a few percent for any reasonable choice of l from 10^3 to 10^6 cm. In the present circumstance, we find $l = 4R_g/(1+z) = 2.4 \times 10^4$ cm. This illustrates the extreme curvature of spacetime as the corresponding coordinate interval of the distant observer is $\delta r \sim 10$ cm.

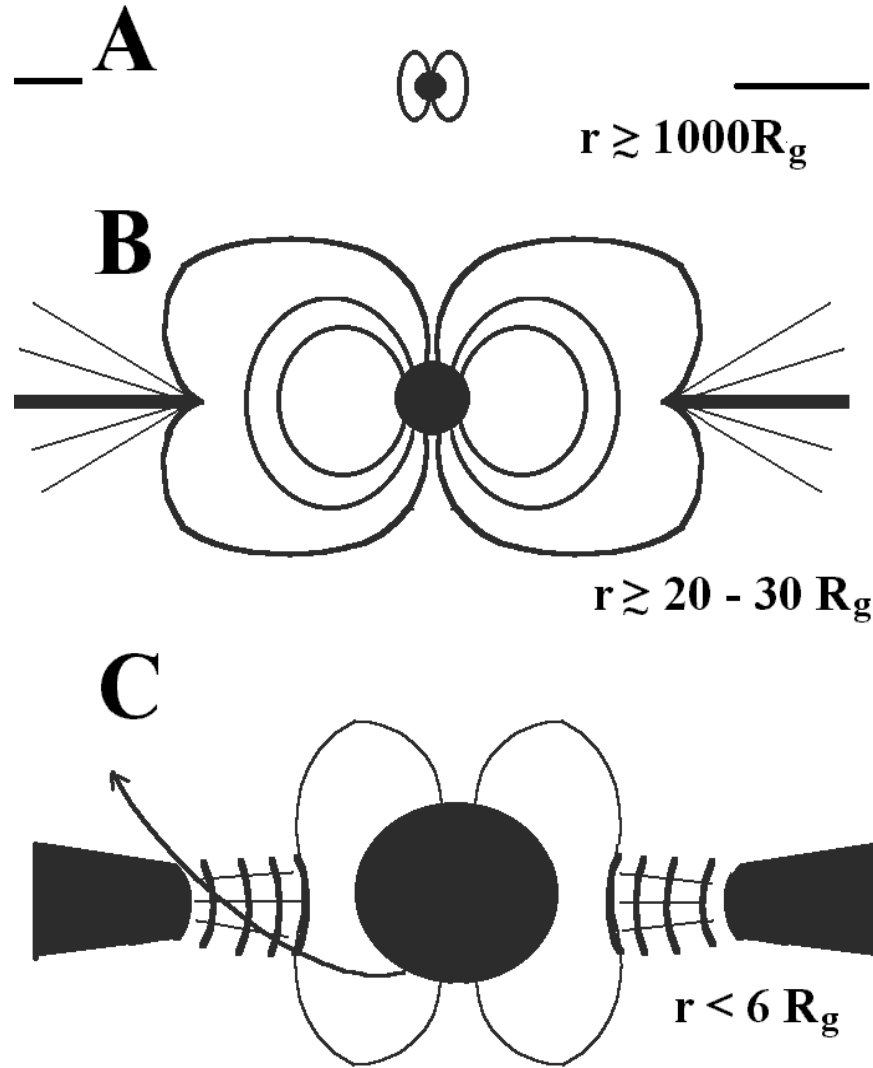


FIG. 1.— MECO Spectral States: **A quiescent:** Inner disk ablated, low accretion rate to inner ablation radius $\sim 10^9 - 10^{10} \text{ cm}$ generates optical emissions. Magnetic dipole radiation produces hard power-law x-ray spectrum. Cooling NS or quiescent MECO emissions may be visible. **B. Low state:** Thin, gas pressure dominated inner disk has a radius between the light cylinder and co-rotation radii. Disk winds and jets are driven by the magnetic propeller. A hard spectrum is produced as most soft x-ray photons from the disk are Comptonized by either outflow or corona. Outflows of electrons on open magnetic field lines produce synchrotron radiation. Most of the outer disk is shielded from the magnetic field of the central object as surface currents in the inner disk change the topology of the magnetopause. **C: High state:** Once the inner disk is inside the co-rotation radius, the outflow and synchrotron emissions subside. A boundary layer of material beginning to co-rotate with the magnetosphere may push the magnetopause to the star surface for NS or inside r_{ms} for MECO, where a supersonic flow plunges inward until radiation pressure stabilizes the magnetopause. Plasma continues on to the MECO surface via interchange instabilities. The MECO photosphere radiates a bright ‘ultrasoft’ thermal component. Bulk comptonization of many photons on spiral trajectories crossing the disk produces a hard x-ray spectral tail.